

Collapse of layer dimerization in the photo-induced hidden state of 1T-TaS₂

Quirin Stahl,¹ Maximilian Kusch,¹ Florian Heinsch,^{2,1} Gaston Garbarino,³ Norman Kretzschmar,³ Kerstin Hanff,⁴ Kai Rossnagel,^{4,5,6} Jochen Geck,^{1,7} and Tobias Ritschel¹

¹*Institut für Festkörper- und Materialphysik, Technische Universität Dresden, 01062 Dresden, Germany*

²*Institute of Radiation Physics, Helmholtz-Zentrum Dresden-Rossendorf, 01328 Dresden, Germany*

³*ESRF, The European Synchrotron, 38000 Grenoble, France*

⁴*Institut für Experimentelle und Angewandte Physik,*

Christian-Albrechts-Universität zu Kiel, 24098 Kiel, Germany

⁵*Ruprecht-Haensel-Labor, Christian-Albrechts-Universität zu Kiel und Deutsches Elektronen-Synchrotron DESY, 24098 Kiel und 22607 Hamburg, Germany*

⁶*Deutsches Elektronen-Synchrotron DESY, 22607 Hamburg, Germany*

⁷*Würzburg-Dresden Cluster of Excellence ct.qmat,*

Technische Universität Dresden, 01062 Dresden, Germany

Photo-induced switching between collective quantum states of matter is a fascinating rising field with exciting opportunities for novel technologies. Presently very intensively studied examples in this regard are nanometer-thick single crystals of the layered material 1T-TaS₂, where picosecond laser pulses can trigger a fully reversible insulator-to-metal transition (IMT). This IMT is believed to be connected to the switching between metastable collective quantum states, but the microscopic nature of this so-called hidden quantum state remained largely elusive up to now. Here we determine the latter by means of state-of-the-art x-ray diffraction and show that the laser-driven IMT involves a marked rearrangement of the charge and orbital order in the direction perpendicular to the TaS₂-layers. More specifically, we identify the collapse of inter-layer molecular orbital dimers, which are a characteristic feature of the insulating phase, as a key mechanism for the non-thermal IMT in 1T-TaS₂, which indeed involves a collective transition between two truly long-range ordered electronic crystals.

The layered transition metal dichalcogenides (TMDs) form a vast class of materials hosting diverse non-trivial quantum phenomena such as spin-valley polarization [1], Ising-superconductivity [2] or intertwined electronic orders [3, 4]. All these intriguing electronic effects along with the natural suitability of TMDs for the preparation of quasi two-dimensional (2D) nano-sheets render them highly appealing for next-generation technologies [5–8].

1T-TaS₂ is a particularly interesting and extensively studied TMD in which external tuning parameters like temperature, pressure or chemical substitution span a particularly complex electronic phase diagram. Apart from several charge density waves (CDWs) this phase diagram also features pressure-induced superconductivity and a so-called Mott-phase, which stands out due to its semiconducting electronic transport properties [3, 9].

Remarkably, besides the aforementioned states that can be reached in thermal equilibrium, femto to picosecond optical or electrical pulses can launch a non-equilibrium IMT into a previously hidden and persistent metallic CDW-state [7, 10, 11]. The discovery of this so-called hidden CDW (HCDW) has sparked wide excitement as it might provide a new platform for memory device applications. Accordingly, in recent years, a significant number of experimental and theoretical studies aimed at pinning down the microscopic mechanism of this non-equilibrium IMT that is believed to be connected to a reorganization of the CDW-order. However, despite significant efforts to determine the microscopic processes underlying this novel IMT have been made [12–17], a

clear picture remains elusive.

In this article we address this open issue directly by means of high-resolution synchrotron x-ray diffraction (XRD) in combination with laser pumping. Our experiments enable examination of the laser-driven transition and in-particular the HCDW-order in 1T-TaS₂ nano-sheets with great sensitivity and in all three spatial directions. In this way we show that ultra-short laser pulses drive a collapse of the inter-layer dimerization present in thermal equilibrium, revealing the key physical process behind the laser-driven IMT of 1T-TaS₂.

At ambient pressure and at temperatures below ≈ 180 K a commensurate charge density wave (CCDW) develops within the layers of 1T-TaS₂, which is characterized by the formation of star-of-David (SOD) shaped clusters containing 13 Ta-sites arranged in a $\sqrt{13} \times \sqrt{13}$ superlattice (cf. Fig 1 (a,b)). The periodic lattice distortion (PLD) associated with a CDW has a larger periodicity than the underlying crystal lattice and becomes visible in XRD through the appearance of characteristic superlattice reflections which are typically $\approx 10^2$ times weaker than the Bragg reflections stemming from the average structure. For the CCDW these reflections occur at the commensurate q-vectors $q_1^C = (\sigma_1^C, \sigma_2^C, l)$ and $q_2^C = (-\sigma_2^C, \sigma_1^C + \sigma_2^C, l)$ with $\sigma_1^C = 3/13$ and $\sigma_2^C = 1/13$ [18, 19]. The superlattice structure of the CCDW is very well ordered within the *ab*-plane which translates into sharp superlattice reflections in the *hk*-plane. However, in the direction perpendicular to the S-Ta-S-layers the CDW order is subject to partial dis-

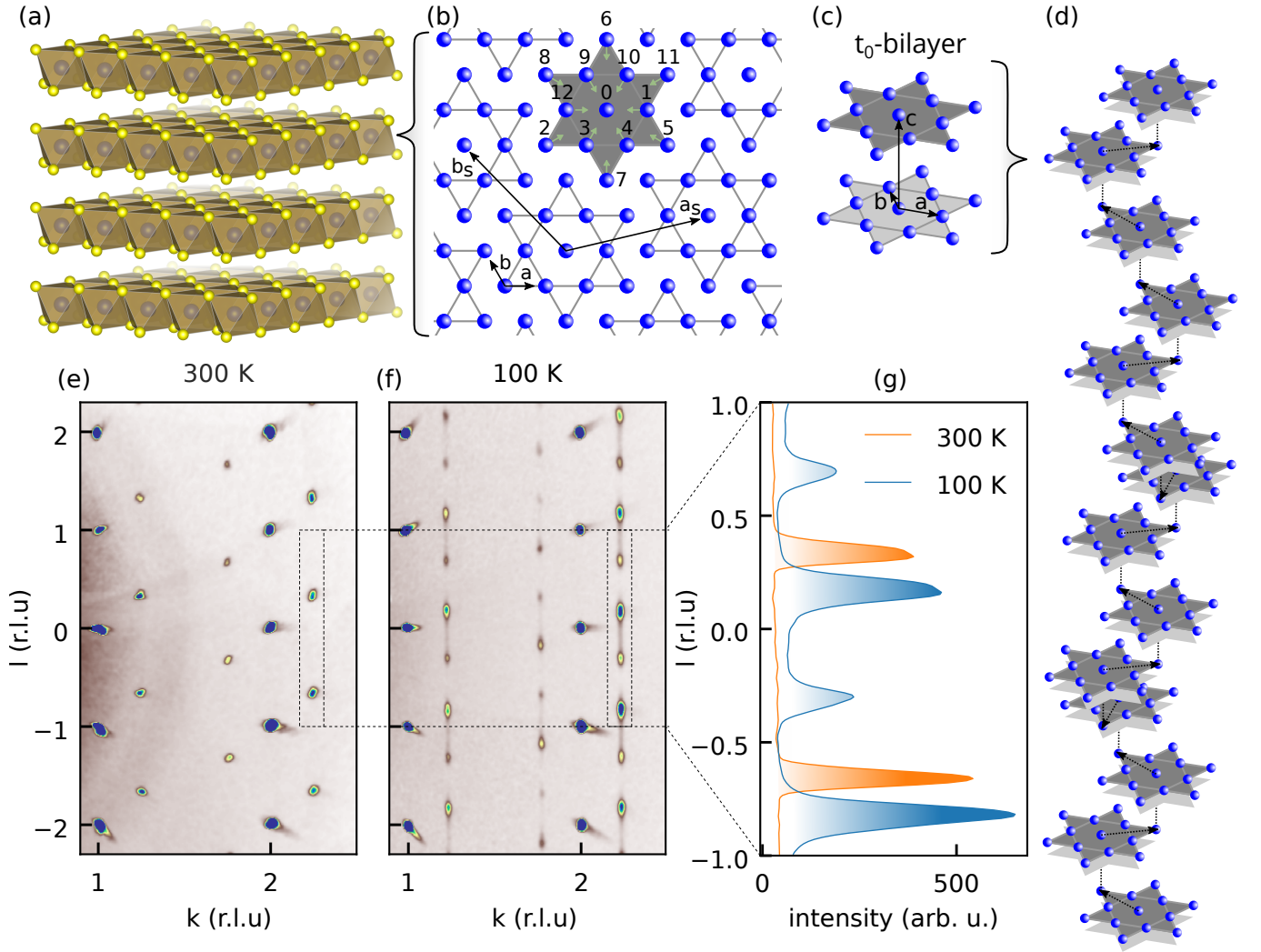


FIG. 1. **Structure and CDW layer stacking in 1T-TaS₂.** (a) The layered host structure of 1T-TaS₂ comprises S-Ta-S layers (Spacegroup: $P\bar{3}m1$). (b) The structural key feature of the C and NCCDW are star-of-David shaped (SOD) clusters containing 13 Tantalum sites formed by an inward displacement (green arrows) of 12 Ta ions (labels 1...12) towards the central Ta ion (label 0). The SOD themselves form a $\sqrt{13} \times \sqrt{13}$ -superlattice with in-plane lattice vectors a_s and b_s . (c) and (d) The partially disordered stacking of the CCDW at low temperatures is dominated by t_0 bilayers (c) which by themselves are stacked with a vector randomly drawn from the three symmetry equivalent vectors \mathbf{t}_7 , \mathbf{t}_8 and \mathbf{t}_{11} (d). The t_0 bilayers are illustrated as gray SODs in (d). (e) and (f): Reciprocal space maps parallel to the kl -plane (integration thickness perpendicular to the plane: 0.3 r.l.u) for $T=300$ K (e: NCCDW) and $T=100$ K (f: CCDW). (g) Intensity profile of the superlattice reflections along the l -direction for CCDW (blue) and NCCDW (orange). The double-peak feature is the key fingerprint for the t_0 bilayers present in the CCDW.

order among the 13 possible two-layer stacking arrangements labeled as $t_0 \dots t_{12}$ corresponding to the 13 Ta-sites within one star-of-David cluster (cf. Fig. 1 (b)).

Due to this disorder in one direction the superlattice reflections form diffuse stripes along the l -direction rather than sharp peaks. The intensity distribution along these stripes has a characteristic two-peak structure (see Fig. 1 (f,g)). A careful analysis of the diffuse-scattering reveals that the 3D CDW-order in 1T-TaS₂ at low temperatures is given by a stacking in which bilayers obeying the t_0 -stacking occur, as illustrated in Fig. 1 (e).

These bilayers are arranged in a stacking sequence, where the stacking vector between two adjacent bilayers is randomly chosen from the three symmetry equivalent vectors \mathbf{t}_7 , \mathbf{t}_8 and \mathbf{t}_{11} , which is schematically depicted in Fig. 1 (d) [20–23].

It should be noted that merely the superlattice reflections show diffuse scattering stripes while the Bragg-peaks remain sharp indicating the absence of more conventional stacking faults in the average structure.

The CCDW phase is also often referred to as the Mott-phase because its unusual semiconducting trans-

port properties are widely believed to stem from Mott-Hubbard type electron-electron correlations [24]. But this paradigm is currently under intense debate as several studies find that the CDW-stacking in the OP-direction has a marked influence on the low-energy electronic structure. In fact, the CDW-stacking can as well drive the formation of a charge excitation gap at the Fermi energy and, hence, yield the observed semiconducting transport behavior. The crucial ingredient for the stacking-induced gap-formation seems to be the occurrence of the t_0 -bilayers [4, 23, 25, 26].

Rising the temperature or applying external pressure transforms the CCDW into a so-called nearly commensurate CDW (NCCDW), accompanied by a significant metallization of the sample. The NCCDW is structurally characterized by the formation of a well-ordered network of defects – so-called discommensurations – within the $\sqrt{13} \times \sqrt{13}$ -superlattice of SODs [19, 27, 28]. This in-plane modification of the CDW structure takes place on a length-scale of about 70 Å and is accompanied with a marked rearrangement of the CDW order in the out-of-plane direction. In XRD the fingerprints of the NCCDW are given by a slight shift of the q -vectors to $q_1^{NC} = (\sigma_1^{NC}, \sigma_2^{NC}, 1/3)$ and $q_2^{NC} = (-\sigma_2^{NC}, \sigma_1^{NC} + \sigma_2^{NC}, -1/3)$ with $\sigma_1^{NC} = 0.248$ and $\sigma_2^{NC} = 0.068$ [19], along with the appearance of strong higher-order superlattice reflections owing to the domain-like structure imposed by the discommensurations. Instead of the diffuse stripes along the l -direction which occur for the CCDW, the superlattice reflections of the NCCDW are sharp and centered at $l_{NC} = \pm 1/3$, indicating a well-ordered CDW stacking with a periodicity of three times the interlayer distance and the absence of the t_0 bilayers (cf. Figure 1 (e,g)). Although the microscopic mechanism of the IMT associated with the NCCDW-CCDW transition is far from being established, there is increasing evidence that exactly this rearrangement of the CDW stacking plays a crucial role [23, 26].

Since the photoinduced HCDW is also accompanied by a metallization of 1T-TaS₂ the question arises whether or not the CDW stacking in the OP-direction is affected by this transition, too.

RESULTS

In order to address exactly this question concerning the CDW structure and in particular the CDW stacking in the out-of-plane direction of the HCDW, we performed XRD on thin exfoliated samples of 1T-TaS₂ in which we induced the HCDW by means of a single 1.6 ps pulse from a Ti-sapphire laser at the beamline ID09 at the ESRF (see methods section for details).

The key results of these experiments are summarized in Fig. 2, which show reconstructed reciprocal space maps

for a switching cycle

$$(\text{NCCDW}) \xrightarrow{\text{cooling}} (\text{CCDW}) \xrightarrow{\text{laser pulse}} (\text{HCDW})$$

of a thin flake 1T-TaS₂ sample. Figures 2 (a-c) illustrate the changes of the in-plane components of the superlattice reflections by projecting the diffraction pattern along the l -direction within a range of $-1/3 < l < 1/3$ onto the $hk0$ -plane, i. e. the plane parallel to the S-Ta-S layers. In order to visualize the changes of the out-of-plane component and the peak profile of superlattice reflections in the OP-direction, we project the diffraction pattern onto the $0kl$ -plane within a h -range of $-0.1 < h < 0.1$ in Fig. 2

Starting at room temperature, we observe the characteristic higher order superlattice reflections in the projection onto the hk -plane indicating the presence of ordered discommensurations in the NCCDW (see Fig. 2 (a)). The IP-parameters of the q -vector $\sigma_1^{NC} = 0.245 \pm 0.002$ and $\sigma_2^{NC} = 0.067 \pm 0.002$ are in excellent agreement with the values obtained for single crystal bulk samples [19, 29]. Also for these thin flakes the NCCDW superlattice reflections are sharp along the l -direction and appear at $l = \pm 1/3$ indicating the tripling of the unit cell in the out-of-plane direction (Fig. 2 (g)). After cooling the sample to 4 K the diffraction pattern changed such that the higher order superlattice reflections vanish as the in-plane components of the q -vector assume the commensurate values $\sigma_1^C = 3/13$ and $\sigma_2^C = 1/13$. (see Fig. 2 (b)). As can be observed in Fig. 2 (e,h), the superlattice peaks exhibit the characteristic diffuse stripes with the double peak structure along the l -direction. This is also found for bulk single crystals and identifies the peculiar CDW-stacking of the CCDW described above. We can therefore conclude that our thin exfoliated flakes of 1T-TaS₂ and bulk single crystals of 1T-TaS₂ develop the same in- and out-of-plane CDW-order.

As the diffraction pattern unambiguously disclosed the formation of the CCDW at low temperatures, we continued by applying a single 1.6 ps long laser pulse with a wavelength of 800 nm and a pulse energy of 0.18 μJ which corresponds to a fluence in the range of 1 mJ/cm² while keeping the nominal sample temperature at 4 K. According to previous reports this procedure creates the HCDW [7]. Indeed, in response to the photo-excitation the diffraction pattern changes very clearly and the higher order superlattice peaks in the projection onto the hk -plane appear again. This is qualitatively similar to the NCCDW at room temperature, yet with somewhat different in-plane components of the q -vector, namely $\sigma_1^H = 0.243 \pm 0.002$ and $\sigma_2^H = 0.070 \pm 0.003$ and, hence, a smaller discommensurability $\delta = |q_H^{\parallel} - q_C^{\parallel}|$ as compared to the NCCDW (see also Table I for a comparison of the in-plane q -vector parameters). Even more striking is that the peak profile in the l -direction becomes sharp again and shifts back to $l = \pm 1/3$. In other words, the double peak structure, characteristic for the t_0 -bilayers in the

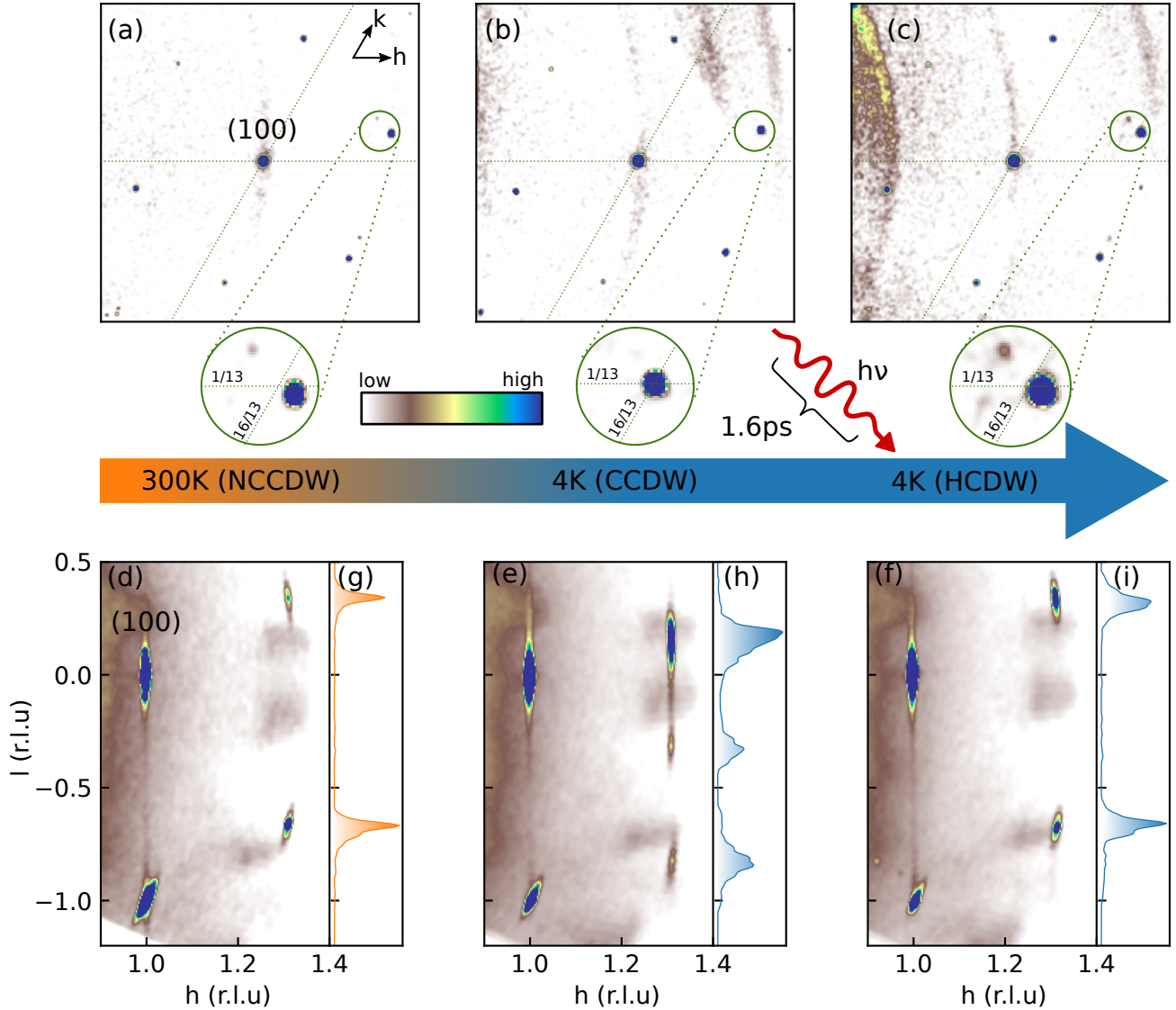


FIG. 2. **Photo-induced changes of the XRD from an thin flake of 1T-TaS₂.** Reciprocal space maps parallel to the $hk0$ -plane (integration thickness perpendicular to the plane: $\delta l = 2/3$ r.l.u.) for the NCCDW at room temperature (a), the CCDW at $T = 4$ K (b) and the photo-induced HCDW at the same temperature $T = 4$ K. The characteristic occurrence of strong higher order superlattice reflections due to the in-plane discommensurations network is clearly observable for the NCCDW (a) and the HCDW (c). Reciprocal space maps parallel to the $0kl$ -plane (integration thickness perpendicular to the plane: $\delta k = 0.3$ r.l.u.) are shown in (d-f) for NCCDW, CCDW and HCDW, respectively. The extracted intensity distribution of the superlattice reflections along the l -direction clearly shows the well defined sharp spots for the NCCDW (g), the characteristic diffuse double peak feature for the CCDW (h) and the vanishing of the diffuse scattering for the photo-induced HCDW.

CCDW, disappears upon laser pumping. This strong effect of the laser pump pulse can be clearly observed in Figs. 2 (e,f) and Figs. 2 (h,i).

For all three states the superlattice peak widths within the plane are always comparable to the width of the Bragg peaks, indicating that the IP-superstructure remains long-range ordered. Note that the XRD data for the HCDW has been taken several seconds after the laser pulse hit the sample, meaning that the sample tem-

perature is well-defined at $T = 4$ K. Accordingly, the CCDW would be the thermodynamic stable state of the system under these conditions, which demonstrates the metastable nature of the HCDW. Notwithstanding, the resolution limited peak width observed here, clearly show that non-equilibrium process driven by the 1.6 ps laser pulse results in a truly long-ranged ordered HCDW-state.

The system flips back to the CCDW when the sample is warmed up to about 40 K in accordance with previ-

state	σ_1 (r.l.u.)	σ_2 (r.l.u.)	δ (10^{-2} r.l.u)	ϕ (deg)	$ q $ (r.l.u)
C	3/13	1/13	0	13.898	0.277
H	0.243 ± 0.002	0.070 ± 0.003	1.06 ± 0.16	12.3 ± 0.3	0.284 ± 0.002
NC	0.245 ± 0.002	0.067 ± 0.002	1.32 ± 0.16	11.9 ± 0.3	0.284 ± 0.002

TABLE I. Parameters of the in-plane q -vector for CCDW, HCDW and NCCDW. σ_1 and σ_2 are the in-plane components. δ is the incommensurability $\delta = |q_H^\parallel - q_C^\parallel|$. ϕ is the angle of the in-plane q -vector with respect to the reciprocal a^* axis and $|q|$ is the length of the in-plane q -vector.

ous resistivity measurements [7]. It is important to realize that this temperature is significantly lower than that of the temperature driven CCDW-NCCDW transition, which is at a temperature of about 220 K.

We also mention that for some samples we observed an incomplete photo-induced switching from the CCDW to the NCCDW, resulting in the simultaneous occurrence of both types of corresponding superlattice reflections. This observation, which we attribute to a slight mismatch of sample size, laser spot size and x-ray spot size, demonstrates that both types of long-range orders – the CCDW and the HCDW – can macroscopically coexist in the same sample.

We also studied the effect of the laser pulse fluence on the induced HCDW by increasing the laser power: Most importantly, the sharpening of the superlattice reflection along the l -direction remains unaffected by changing the laser pulse fluence which means that the breakdown of the \mathbf{t}_0 bilayers fully takes place as soon as the switching threshold is reached. Further we found evidence that the in-plane q -vector of the HCDW slightly shifts towards the position of the room temperature NCCDW in-plane q -vector with increasing laser fluence. This trend is consistent with pump-probe electron diffraction experiments at higher temperatures [30].

DISCUSSION

We now turn the discussion towards the origin of the metallicity of the HCDW in the light of our observations. Our data reveal that the metallization in the HCDW goes along with a reordering of the CDW in the out-of-plane direction as well as the formation of discommensurations. Recent studies based on density functional theory (DFT) indeed provide strong evidence that the changes in the out-of-plane direction play an important role for the IMT [4, 23, 26]. More specifically, these studies identify a key feature responsible for the insulating properties of the CCDW, namely the formation of \mathbf{t}_0 bilayers characteristic for the CCDW stacking along the out-of-plane direction. Our experimental data show that these bilayers indeed collapse in response to the picosecond laser pulse as can be unambiguously seen from the vanishing double peak structure in the intensity distribution of the superlattice reflections along the l -direction (cf. Fig-

ure 2 (d-i)). The same breakdown of the \mathbf{t}_0 bilayers also happens as a function of temperature or pressure at the CCDW-NCCDW transition, which is also accompanied by a marked change of the electrical resistivity. We therefore conclude that the rearrangement of the CDW structure in the out-of-plane direction involving the collapse of the \mathbf{t}_0 -bilayers lies at the core of the photo-induced IMT.

The formation of the \mathbf{t}_0 -bilayers is closely related to the hybridization between the orbitally ordered CDW layers, where each SODs represents one quasi-molecular orbital. In other words, the CCDW phase is characterized by a dimerization of SODs in the out-of-plane direction, i.e., the formation interlayer dimer-bonds [4, 23, 26]. According to our observations, photo-excitation breaks exactly these interlayer dimers. Since this primarily is an electronic process involving orbital degrees of freedom, the latter is indeed likely to proceed on ultra-fast electronic time scales, in agreement with previous time-resolved experiments[31–34].

We also would like to stress that the HCDW structure in our experiments is always long range ordered throughout the thin sample. In contrast, recent STM experiments on the HCDW show a strongly disordered network of discommensurations at the surface [17]. The sharp superlattice reflections and the absence of significant diffuse scattering in our bulk sensitive XRD measurements of the HCDW instead imply that the discommensurations form a very well ordered network very similar to the NCCDW at room temperature. This comparison therefore implies that the photo-induced processes at the surface and in the bulk are different, which is certainly relevant with respect to the down-scaling of the sample thickness for possible technological applications.

Regarding the photo-induced IMT in the bulk, our data reveal a marked similarity between the HCDW and the NCCDW. In spite of these clear similarities, it has been argued previously that the NCCDW and HCDW are distinct states because they differ in their electrical resistivity and the frequency of the amplitude mode of the CDW [7, 10]. Indeed, besides the aforementioned similarities of the HCDW and the NCCDW, the present XRD-study uncovers also an important difference between these two states, namely a different density of discommensurations. Our measurements show that the in-plane incommensurability δ of the HCDW q -vector is

smaller than that of the room temperature NCCDW (see Table I), implying a smaller density of discommensurations in the HCDW as compared to the room temperature NCCDW [27, 29]. It is likely that salient features of the discommensurations network, such as the concentration of discommensurations, alter the transport properties as well as the frequency of the amplitude mode.

In conclusion, we employed synchrotron XRD in combination with picosecond laser-pumping to uncover the structure of the photo-induced HCDW in 1T-TaS₂ nanosheets. Our data disclose a key mechanism of the photo-induced IMT: The collapse of interlayer dimers, which are a characteristic feature of the insulating CCDW. Thus, the present study implies that the reorganization of the orbitally ordered layers in the out-of-plane direction rather than in the in-plane direction lies at the core of the marked transport anomalies in 1T-TaS₂. On a more general level, the case at hand illustrates in a most striking manner that out-of-plane correlations between the layers in Van der Waals materials can play a crucial role for their physical properties. This is not just a mere complication. It rather provides a unique way to control the electronic properties of such materials in the few layer limit.

A very intriguing and surprising feature of the studied case is that a single picosecond laser pulse can trigger a transition between two very complex and truly long-range ordered electronic states, which are the endpoints of the photo-induced IMT. How this transition proceeds on atomic length and electronic time scales still remains an open and very fascinating puzzle. To ultimately clarify and fully understand this unusual collective electronic phenomenon will however require further time-resolved experiments.

METHODS

Sample preparation

The high-quality 1T-TaS₂ bulk single crystals used for the present study were grown by the iodine vapor transport method as described in Ref. 35. The thin films with a thickness in order of about 50 nm and typical lateral dimensions up to 200 μm were prepared by mechanical exfoliation. The exfoliated samples were transferred onto standard TEM silicon nitride windows with 200 nm thickness.

XRD measurements and laser excitation

The bulk single crystal XRD data at room temperature and 100 K were measured at a Bruker APEXII diffractometer.

The XRD experiments on the exfoliated 1T-TaS₂ samples were performed at the beamline ID09 of the European Synchrotron Radiation Facility. The TEM silicon nitride window with the exfoliated 1T-TaS₂ samples were mounted on the cold finger of a specially designed continuous He-flow cryostat with Mylar windows which are transparent for both the optical laser radiation and the 18 keV x-ray radiation. The cryostat was attached to a single rotation axis. Photo-excitation of the exfoliated 1T-TaS₂ samples was achieved by means of a single pulse from an optical Ti-sapphire laser with a wavelength of 800 nm and a pulse duration of 1.6 ps. The laser spot size on the sample was about 400 μm (FWHM) while the x-ray beam spot size was about 60 × 100 μm². XRD single crystal datasets from the samples were collected using a Rayonix MX170 detector in transmission geometry. All data sets contain 120 frames with 0.5 deg scan width over a sample rotation of 60 deg. From these data sets we calculated reciprocal space maps as shown in Figure 1 and 2 using the CrysAlis Pro software package [36].

ACKNOWLEDGEMENTS

This research has been supported by the Deutsche Forschungsgemeinschaft through the SFB 1143, the Wzburg-Dresden Cluster of Excellence EXC 2147 (ct.qmat), the Graduate School GRK 1621, and Grant No. RI 2908/1-1. We also gratefully acknowledge the support provided by the DRESDEN-concept alliance of research institutions, thank T. Woike and M. Wulff for helpful discussions and the ESRF for providing the beamtime at ID09.

-
- [1] D. Xiao, G.-B. Liu, W. Feng, X. Xu, and W. Yao, *Physical Review Letters* **108** (2012), 10.1103/physrevlett.108.196802.
 - [2] X. Xi, Z. Wang, W. Zhao, J.-H. Park, K. T. Law, H. Berger, L. Forró, J. Shan, and K. F. Mak, *Nat. Phys.* **12**, 139 (2015).
 - [3] B. Sipoš, A. F. Kusmartseva, A. Akrap, H. Berger, L. Forro, and E. Tutis, *Nat Mater* **7**, 960 (2008).
 - [4] T. Ritschel, J. Trinckauf, K. Koepf, B. Büchner, M. v. Zimmermann, H. Berger, Y. I. Joe, P. Abbamonte, and J. Geck, *Nat Phys* **11**, 328 (2015).
 - [5] B. Radisavljevic, A. Radenovic, J. Brivio, V. Giacometti, and A. Kis, *Nat Nano* **6**, 147 (2011).
 - [6] D. Jariwala, V. K. Sangwan, L. J. Lauhon, T. J. Marks, and M. C. Hersam, *ACS Nano* **8**, 1102 (2014), <http://dx.doi.org/10.1021/nm500064s>.
 - [7] L. Stojchevska, I. Vaskivskiy, T. Mertelj, P. Kusar, D. Svetin, S. Brazovskii, and D. Mihailovic, *Science* **344**, 177 (2014).
 - [8] M. Yoshida, R. Suzuki, Y. Zhang, M. Nakano, and Y. Iwasa, *Sci. Adv.* **1**, e1500606 (2015).

- [9] J. Wilson, F. Di Salvo, and S. Mahajan, *Advances in Physics* **24**, 117 (1975).
- [10] I. Vaskivskiy, J. Gospodaric, S. Brazovskii, D. Svetin, P. Sutar, E. Goresnik, I. A. Mihailovic, T. Mertelj, and D. Mihailovic, *Science Advances* **1** (2015), 10.1126/sciadv.1500168.
- [11] M. J. Hollander, Y. Liu, W.-J. Lu, L.-J. Li, Y.-P. Sun, J. A. Robinson, and S. Datta, *Nano Letters* **15**, 1861 (2015), pMID: 25626012, <http://dx.doi.org/10.1021/nl504662b>.
- [12] L. L. Guyader, T. Chase, A. H. Reid, R. K. Li, D. Svetin, X. Shen, T. Vecchione, X. J. Wang, D. Mihailovic, and H. A. Dürr, *Structural Dynamics* **4**, 044020 (2017).
- [13] R. Hovden, P. Liu, N. Schnitzer, A. W. Tsen, Y. Liu, W. Lu, Y. Sun, and L. F. Kourkoutis, *Microscopy and Microanalysis* **24**, 387 (2018).
- [14] L. Ma, C. Ye, Y. Yu, X. F. Lu, X. Niu, S. Kim, D. Feng, D. Tomanek, Y.-W. Son, X. H. Chen, and Y. Zhang, *Nat Commun* **7**, 10956 (2016).
- [15] D. Cho, S. Cheon, K.-S. Kim, S.-H. Lee, Y.-H. Cho, S.-W. Cheong, and H. W. Yeom, *Nat Commun* **7**, 10453 (2016).
- [16] D. Cho, G. Gye, J. Lee, S.-H. Lee, L. Wang, S.-W. Cheong, and H. W. Yeom, *Nat. Commun.* **8** (2017), 10.1038/s41467-017-00438-2.
- [17] Y. A. Gerasimenko, I. Vaskivskiy, and D. Mihailovic, 1704.08149v2.
- [18] R. Brouwer and F. Jelinek, *Physica B+C* **99**, 51 (1980).
- [19] A. Spijkerman, J. L. de Boer, A. Meetsma, G. A. Wieggers, and S. van Smaalen, *Phys. Rev. B* **56**, 13757 (1997).
- [20] M. B. Walker and R. L. Withers, *Phys. Rev. B* **28**, 2766 (1983).
- [21] K. Nakanishi and H. Shiba, *Journal of the Physical Society of Japan* **53**, 1103 (1984).
- [22] S. Tanda, T. Sambongi, T. Tani, and S. Tanaka, *Journal of the Physical Society of Japan* **53**, 476 (1984).
- [23] T. Ritschel, H. Berger, and J. Geck, *Phys. Rev. B* **98** (2018), 10.1103/physrevb.98.195134.
- [24] e. Tosatti and p. fazekas, *Le Journal de Physique Colloques* **37**, C4 (1976).
- [25] Y. Ge and A. Y. Liu, *Phys. Rev. B* **82**, 155133 (2010).
- [26] S.-H. Lee, J. S. Goh, and D. Cho, *Physical Review Letters* **122** (2019), 10.1103/physrevlett.122.106404.
- [27] K. Nakanishi and H. Shiba, *Journal of the Physical Society of Japan* **44**, 1465 (1978), <http://dx.doi.org/10.1143/JPSJ.44.1465>.
- [28] X. L. Wu and C. M. Lieber, *Science* **243**, 4899 (1989).
- [29] T. Ritschel, J. Trinckauf, G. Garbarino, M. Hanfland, M. v. Zimmermann, H. Berger, B. Büchner, and J. Geck, *Phys. Rev. B* **87**, 125135 (2013).
- [30] T.-R. T. Han, F. Zhou, C. D. Malliakas, P. M. Duxbury, S. D. Mahanti, M. G. Kanatzidis, and C.-Y. Ruan, *Science Advances* **1**, e1400173 (2015).
- [31] L. Perfetti, P. A. Loukakos, M. Lisowski, U. Bovensiepen, M. Wolf, H. Berger, S. Biermann, and A. Georges, *New J. Phys.* **10**, 053019 (17pp) (2008).
- [32] S. Hellmann, M. Beye, C. Sohrt, T. Rohwer, F. Sorgenfrei, H. Redlin, M. Kalläne, M. Marczyński-Bühlow, F. Hennies, M. Bauer, A. Föhlich, L. Kipp, W. Wurth, and K. Rossnagel, *Phys. Rev. Lett.* **105**, 187401 (2010).
- [33] S. Hellmann, T. Rohwer, M. Kalläne, K. Hanff, C. Sohrt, A. Stange, A. Carr, M. Murnane, H. Kapteyn, L. Kipp, M. Bauer, and K. Rossnagel, *Nat Commun* **3**, 1069 (2012).
- [34] M. Liggés, I. Avigo, D. Golež, H. Strand, Y. Beyazit, K. Hanff, F. Diekmann, L. Stojchevska, M. Kalläne, P. Zhou, K. Rossnagel, M. Eckstein, P. Werner, and U. Bovensiepen, *Physical Review Letters* **120** (2018), 10.1103/physrevlett.120.166401.
- [35] F. Zwick, H. Berger, I. Vobornik, G. Margaritondo, L. Forró, C. Beeli, M. Onellion, G. Panaccione, A. Taleb-Ibrahimi, and M. Grioni, *Phys. Rev. Lett.* **81**, 1058 (1998).
- [36] “Oxford Diffraction /Agilent Technologies UK Ltd, Yarn-ton, England.”.